Journal of Solid State Chemistry 184 (2011) 2184–2189

Contents lists available at ScienceDirect

Journal of Solid State Chemistry

journal homepage: www.elsevier.com/locate/jssc

Effect of nitrogen-containing groups on enhanced capacitive behaviors of multi-walled carbon nanotubes

Ji-Il Kim, Soo-Jin Park *

Department of Chemistry, Inha University, 253 Nam-gu, Incheon 402-751, South Korea

ARTICLE INFO

Article history:
Received 17 December 2010
Received in revised form
5 April 2011
Accepted 29 May 2011
Available online 12 June 2011

Keywords:
Supercapacitors
Multi-walled carbon nanotubes
Nitrogen
Surface treatment

ABSTRACT

In this work, electrochemical properties of surface treated multi-walled carbon nanotubes (MWNTs) are studied in supercapacitors. Nitrogen and oxygen functional groups containing MWNTs are prepared by urea and acidic treatments, respectively. The surface properties of the MWNTs are confirmed by X-ray photoelectron spectroscopy (XPS) and zeta-potential measurements. The textural properties are characterized by N_2 adsorption/desorption isotherm at 77 K using the BET eqaution, BJH method, and HK method. The electrochemical properties of the MWNTs are accumulated by cyclic voltammetry, impedance spectra, and charge–discharge cycling performance in 1 M H_2SO_4 at room temperature. As a result, the functionalized MWNTs lead to an increase in capacitance as compared with pristine MWNTs. It suggests that the pyridinic and pyridinic-N-oxides nitrogen species have effects on the specific capacitance due to the positive charge, and thus an improved electron transfer at high current loads results, the most important functional groups affecting capacitive behaviors.

1. Introduction

The supercapacitors are promising energy storage devices that store charge species using electrochemically reversible adsorption of ions between the electrolyte and active materials onto electrode interface [1]. In comparison with secondary batteries, supercpacitors are widely used in commercial devices that can be instantaneously charged and discharged, have high power density, are robust to environmental extremities, are non-toxic, and use relatively inexpensive materials. The specific capacitance of the supercapacitors is dependent on the surface area of the electrode and the thickness of the double layer. Carbon materials are candidates for electrodes in supercapacitors due to their high specific surface area and developed pore structure [2–7]. Among the diverse carbon materials, multi-walled carbon nanotubes (MWNTs) are materials that have received tremendous interest and they are being used in a wide variety of applications apart from electrode material [2,4,5,8], because they show many properites, such as controlling pore structures, high conductivity, chemical stability, good polarization, and other beneficial features. These properties make them potentially quite suitable for application in the fabrication on supercapacitors as an electorde. Thus, they are also applied for other energy storage devices such as secondary batteries, fuel cells, hydrogen storage, and so on [9–11].

Although this type of capacitor is used in electronic devices for its excellent power density, recent researches have been motivated by hybrid electric vehicles and portable devices to meet needs such as more power demand and energy density in electrode materials. Current research on improving electrochemical properties has focused on introducing surface functional groups and chemical activation. Unfortunately, adverse effects, such as destruction of surface structure, decrease in electric conductivity, and increase in cost, resulted when the specific surface area of the MWNTs was increased using chemical activation (about 50 F g^{-1}) [7,12].

Various carbon materials, which are suitable active materials for supercapacitors, have surface functional groups containing many heteroatoms, such as oxygen, nitrogen, sulfur, and halogen. Among them, nitrogen functional groups positively affect the capacitive performance; it not only reduced the destruction of the suface structure but also effectively approached toward attaining an increased specific capacitance. Nitrogen-containing carbon materials could be effectively prepared through carbonization using nitrogen-rich carbon precursors, such as polyacrylonitrile, melamine, quinoline pitch, urea, and so on [13–16].

The existence of these functional groups introduces acid-base characteristics [17–19]into MWNTs, which gives rise to faradaic pseudo-capacitive reactions [1]. Pseudo-capacitance in nitrogen-doped carbons has been suggested, but not confirmed, as the oxidation/reduction of negatively charged nitrogen groups located

* Corresponding author. Fax: +82 32 860 8438.
E-mail address: sjpark@inha.ac.kr (S.-J. Park).

0022-4596/$ - see front matter © 2011 Elsevier Inc. All rights reserved.
doi:10.1016/j.jssc.2011.05.038

at the edge of graphene-like layers [20]. In the case of oxygen functionalities, the most documented case is the reversible oxidation/reduction of hydroquinone/quinone groups.

In the present study, we investigated the combined effect of nitrogen- and oxygen-containing functional groups on MWNTs that were prepared using a thermal decompositon method with urea as a nitrogen precursor. Detailed analyses of pore structure allow the investigation of most of the effective pores for a double-layer formation as well as pores in which the pseudo-capacitive interactions take place. Furthermore, the results are discussed with regard to the type of nitrogen and oxygen functionalities, content of nitrogen, interaction of surface functional groups, and pore structure.

2. Experimental section

2.1. Materials and sample preparation

MWNTs produced via chemical vapor depositon (CVD) method were purchased from Nano Solution Co. (Korea, degree of purity: ≥ 95 wt%, diameter: 10–25 nm, length: 10–50 μm). Prior to use, the pristine MWNTs were purified by impregnating them with 5 M HNO_3 for 5 h at room temperature. Subsequently, these were reiteratively filtered and washed by distilled water, and then dried in vacuum oven during 24 h at 120 °C. The MWNTs were treated with urea in ethanol and suspended for 5 h at room temperature, then the samples were evaporated with ethanol and thoroughly dried at 120 °C. The dried samples were thermal decomposed in nitrogen atmosphere at 900 °C and maintained for 1 h. The products were washed out in boiling distilled water to eliminate decomposed urea. In order to confirm the effect of oxygen functionalities, the purified MWNTs were oxidized with H_3PO_4 for 5 h prior to urea treatment. The purified MWNTs are named to as MWNTs, and the pre-oxidization and thermal decomposition with urea are represented by O and U, repectively. Therefore, the UO-MWNTs are MWNTs pre-oxidized, and they are treated with urea and thermally decomposed at 900 °C.

2.2. Characterization

The elemental composition of the MWNTs as a function of surface treatment was confirmed with X-ray photoelectron spectroscopy (XPS) using ESCA LAB MK-II (VG Scientific Co., UK) equipped with a monochromatic Al $K\alpha$ radiation ($h\upsilon = 1486.6$ eV), operated in constant analyzer mode. The survey and high-resolution spectra were measured with the range of 50–200 eV pass energy. The raw XPS spectra peaks were curve-fitted by non-linear least-squares fitting with Gaussian–Lorentzian line shapes using XPS peak fit software, and binding energy (BE) from C_{1S} spectra (BE = 284.6 eV) was collected as a reference. The surface charge of the products was investigated for the influence of surface functional groups using the Zeta-potential measurements (Zeta-Potential Analyzer, Otsuka Electronics Co., Japan) in ethanol in a neutral condition. The zeta potential of each sample was estimated from the electrophoretic mobility using electrophoretic light scattering measurements. The nitrogen full isotherms were measured at 77 K using a gas adsorption analyzer (TriStar 3000, Micromeritics Co.). The samples were out-gassed at 200 °C for 6 h to obtain a residual pressure of less than 10^{-3} Torr. Specific surface areas, the mesopore volume, and the micropore volume of the samples were measured from the Brunauer–Emmett–Teller (BET) equation, BJH method, and *t*-plot method, respectively.

The electrochemical properties of the MWNT electrodes were performed with a potentiostat/galvanostat (IVIUMSTAT, Japan) using a three-electrode system at room temperature in 1.0 M H_2SO_4 as an electrolyte solutions. A three-electrode system includes a working electrode (Glassy carbon electrode), a platinum counter electrode, and a 3.0 M KCl Ag/AgCl reference electrode. Cyclic voltammetry (CV) of MWNT electrodes was performed in the potential range of 0–1.0 V at a scan rate of 5 mV s^{-1}. The electrochemical impedance spectroscopy measurement of the electrode was carried out in a frequency from 10 kHz to 10 mHz with an alternating current of 20 mV amplitude.

The charge–discharge (CD) curves were used a voltage range of 0–0.9 V in the above conditions. The specific capacitance (C) of the electrodes in supercapacitors was calculated from the slope of the following equation:

$$C = (I\Delta t)/(\Delta V m) \quad (1)$$

where C is the capacitance of the cell in farads, I the discharge current in amperes (A), Δt the time of discharge corresponding to the voltage difference (ΔV), and m the mass of active material on the electrodes.

3. Results and discussion

Fig. 1 shows the N_2/77 K adsorption/desorption isotherms of the MWNTs as a function of surface treatment. The isotherms of all specimens indicated between types II and IV according to the IUPAC classification, showing maintenance of mesoporous structures, in spite of applied surface treatments. A previous study [20] suggested that heteroatoms on surfaces limit the improvement of the pore structures. After surface treatment, the amount of volume adsorbed ($cm^3\ g^{-1}$, STP) for the UO-MWNTs were predominantly decreased more than other specimens due to the pore blocking in the MWNTs by functional groups. The pore structural parameters of the specimens are summarized in Table 1. After surface treatment, the specific surface areas, mesopore volume, and total pore volumes are apt to be decreased by surface treatments as a result of destruction of the pore structures. On the other hand, the surface functional group derived from surface treatment suggests that micropore volumes are more slightly increased than pristine MWNTs. Particularly, O-MWNTs and UO-MWNTs have higher micropore volumes than MWNTs and U-MWNTs, respectively. It seems that acidic and urea treatment might tend to lead the blocking mesopore structures.

The micro- (inset) and mesopore size distribution demonstrated in Fig. 2 shows the pore structure of the specimens, which were predominantly mesoporous structures. The mesopore volume of the surface treated MWNTs is shifted to the left side compared with that of MWNTs. It is observed that the pore volume could be strongly influenced by surface treatment. As illustrated Fig. 2 (inset), in the case of surface treated MWNTs, the volume in pores of size between 1.5 and 4.0 nm is increased as compared with pristine MWNTs. As mentioned above, the mesopore of the highest occupied total pore volume is blocked by surface functional groups, after being incorporated with nitrogen and oxygen functional groups.

XPS analysis was also used to determine the chemical species of all the specimens. Table 2 lists the XPS spectra of the MWNTs as a function of surface treatment. The UO-MWNTs show that the atomic concentration of nitrogen functional groups is the highest value among these specimens, however the content of oxygen is decreased. From the results, the oxygen functional groups are not stable in heat treatment at 900 °C. Furthermore, the oxygen functional groups play a role to engage urea into the reactions, these molecules can penetrate deeper into the pore structure of the MWNTs, resulting in more incorporated nitrogen functional groups.

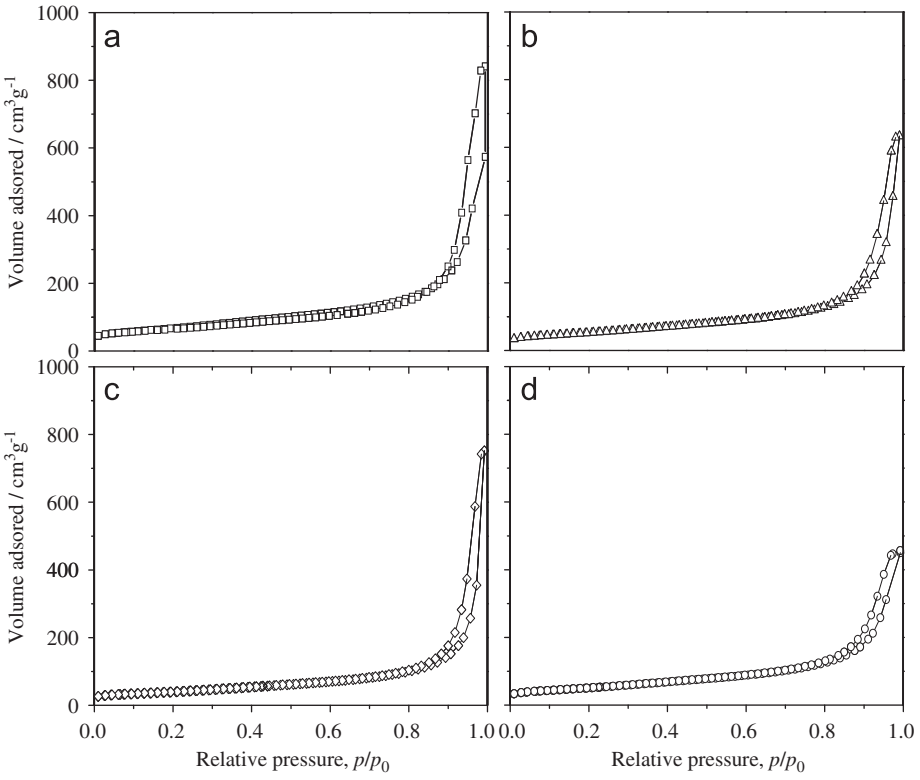

Fig. 1. N_2/77 K adsorption/desorption isotherms of MWNTs (a), O-MWNTs (b), U-MWNTs (c), and UO-MWNTs (d).

Table 1
Porosity parameters of the MWNTs as a function of surface treatment.

Specimens	S_{BET}[a]	V_{mic}[b]	V_{me}[c]	V_t[d]
MWNTs	211	0.011	0.820	0.831
O-MWNTs	168	0.019	0.608	0.627
U-MWNTs	187	0.014	0.658	0.672
UO-MWNTs	155	0.021	0.438	0.459

[a] Specific surface area ($m^2\ g^{-1}$)
[b] Micropore volume ($cm^3\ g^{-1}$)
[c] Mesopore volume ($cm^3\ g^{-1}$)
[d] Total pore volume ($cm^3\ g^{-1}$)

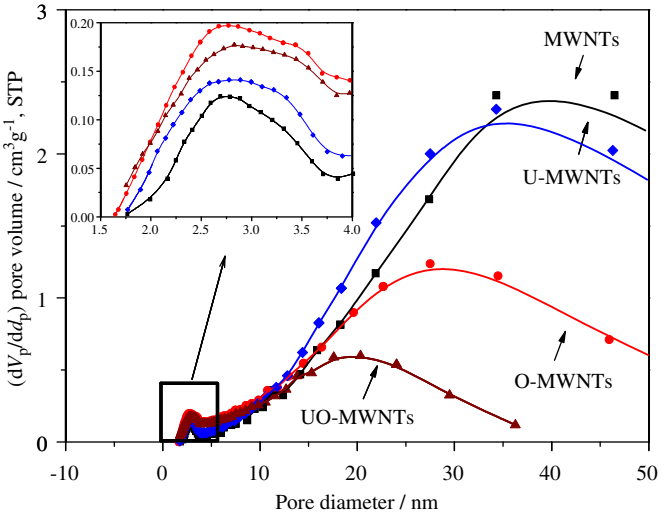

Fig. 2. Micro- (inset) and mesopore size distributions of MWNTs prepared as a function of surface treatment.

Table 2
Elemental composition of the MWNTs as a function of surface treatment.

Specimens	Atomic conc. (%)		
	C	O	N
MWNTs	98.08	1.92	–
O-MWNTs	93.17	6.83	–
U-MWNTs	97.67	1.21	1.12
UO-MWNTs	95.95	1.78	2.27

Fig. 3 displays the N_{1s} spectra of the MWNTs as a function of surface treatment. According to previous literature surveys [15,18,19,21–23], the chemical state of nitrogen functional groups in MWNT surfaces could be assigned to N-6 (pyridinic nitrogen, 398.7 ± 0.3 eV), N-5 (pyrrolic nitrogen and pyridinic nitrogen related to oxygen functionalities, 400.3 eV ± 0.3 eV), N–Q (quaternary nitrogen, 401.4 ± 0.5 eV), and N–X (pyridine-N-oxide, 402–405 eV). Except for N–Q, all nitrogen functional groups were located at the edge of the carbon structure. The fitting curves of N_{1s} spectra for the U-MWNTs and UO-MWNTs were detected at the same binding energies; however, with different relative distribution. The proportions of N-5 and N-X increased with more nitrogen- and oxygen-containing functional groups, indicating the chemical transformation of nitrogen functional groups during the heat treatment. These results demonstrate that N-5 has been chemically shifted into nitrogen functional groups with higher binding energies through the condensation occurring during the heat treatment process [22]. In the case of oxygen, the BEs at 531, 532, and 535 eV represent C=O groups, C–OH, and C–O–C groups, respectively. These results are consistent with previous results in the literature [24–27].

The zeta-potential (ζ) measurements were used to investigate the surface chemistry of different type of solid. The zeta-potential value can be calculated from Smoluchowski's equation (2), which

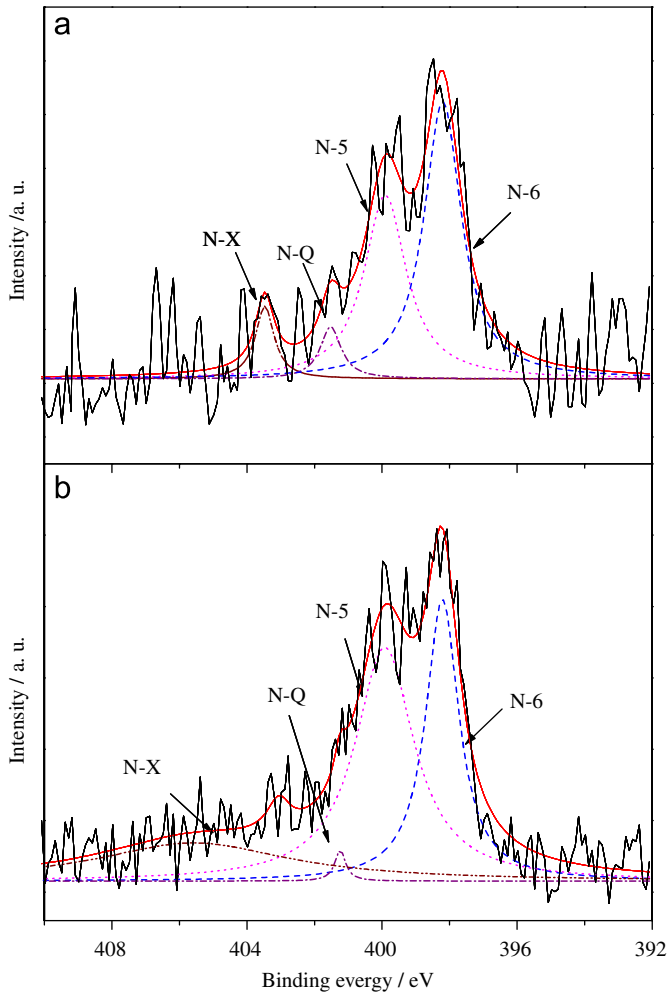

Fig. 3. N_{1S} XPS spectra of U-MWNTs (a) and UO-MWNTs (b).

Table 3
Zeta potential value of the MWNTs as a function of surface treatment.

Specimens	MWNTs	O-MWNTs	U-MWNTs	UO-MWNTs
Zeta potential (mV)	−26.48	−39.56	−17.26	−24.53

is expressed as follows:

$$\zeta = 4\pi\eta U/\varepsilon \quad (2)$$

where η is the coefficient of viscosity of the solvent, ε the dielectric constant of the solvent, U the degree of electrophoresis, and U is given by

$$U = V/E \quad (3)$$

$$V = \Lambda_V \lambda/2n\sin(\theta/2) \quad (4)$$

where E is the electric field, V the mobile velocity, n the refractive index, Λ_V the Doppler-shift, λ the wavelength, and θ the scattering angle.

Table 3 lists the evaluation of the surface charges of all the specimens. The colloidal stability depend on the functional groups, and the specimens were negatively charged in aqueous solution as well as the zeta-potential values obtained for the MWNTs, which are consistent with previously reported data [28,29]. The relatively highest zeta potential value of the O-MWNTs follows as a consequence of reduced energy barrier, which attributed to the inhibition of aggregations. According to Derjaguin–Landau–Verwey–Overbeek (DLVO) theory [30], it describes the relations between the local electric field and the stability of hydrophobic colloids. Thus, these results strongly suggest that the stabilization of the functionalized MWNTs in an aqueous solution is derived from electrostatic force. The suspended functionalized MWNTs are a colloidal system in which the attractive van der Waals forces are counteracted by electrostatic repulsion whereby aggregation is prevented. It can be noted that as zeta-potential value increases, more incorporating oxygen functional groups have an effect on a higher dispersion of MWNTs rather than just urea treatment. For these reasons, the relative contents of nitrogen-containing functional groups on the UO-MWNTs were more than twice as high as the U-MWNTs, in spite of the lowest value of the pore structural parameter among all the specimens, as shown in Table 2.

Fig. 4 displays the CV measured for the electrodes of surface treated MWNTs in 1 M H_2SO_4 as an electrolyte solution at the scan rate of 5 mV s^{-1} from 0 to 1.0 V. All the specimens show pseudo-capacitive peaks at 0.3–0.5 V reflecting a reversible reduction/oxidation of the oxygen functional groups; the UO-MWNTs were closed so it can be defined as shape of an ideal square as well as highest current denstiy value. The deviation from the imaginary rectangular emerged, which is also owing to the pseudo-capacitive effects. An appreciable amount of nitrogen and oxygen functional groups incorporated into the carbon matrix can enhance the wettability between the electrolyte and electrode materials, resulting in the pseudo-capacitive effect. This suggests that the pseudo-capacitive effect was largely influenced by nitrogen and oxygen functional groups on MWNTs.

Nyquist plots represent the frequency responses of the specimens, which show the conductive properties of the MWNTs as shown in Fig. 5. Generally, the high-frequency region represents the sum of the internal resistance of the carbon material, electrolyte resistance, and contact resistance between the working electrode and the current collector. In addition, the imaginary part of the impedance spectra at a low frequency demonstrates capacitive behaviors of the electrode and approaches a vertical line in an ideal capacitive performance [1]. Note that all spectra contain a distorted semicircle in the high frequency region due to porosity of the electrode and a vertical linear part at the low frequency owing to a diffusion-controlled doping/undoping of anions, resulting from Warburg behavior [31]. On the other hand, the Nyquist plots for surface treated MWNTs were quite different

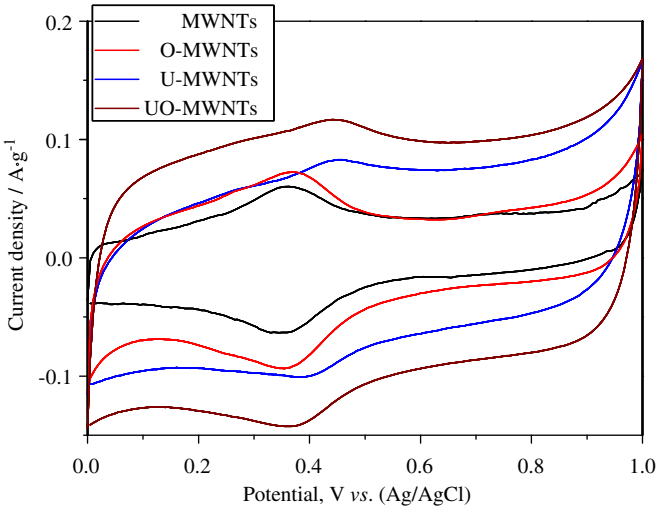

Fig. 4. Cyclic voltammograms of MWNTs-based on electrodes at the scan rate of 5 m Vs^{-1} in 1 M H_2SO_4.

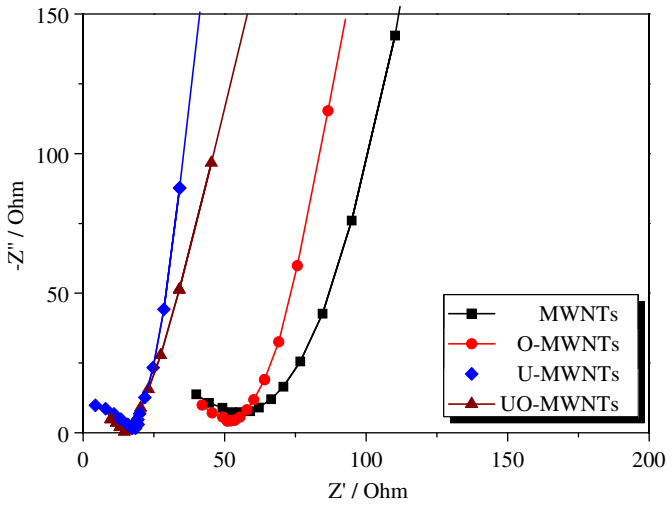

Fig. 5. Impedance spectra of surface treated MWNT electrodes for supercapacitors.

from the pristine MWNTs. The internal resistance of the UO-MWNTs was estimated at a lower value than other samples, suggesting a lowering of the intrinsic resistance of the electrode. As a result, increasing electric conductivity depends on the contents of nitrogen, which is attributed to more rapid charge transfer of nitrogen-containing MWNTs due to the improved wettability between the electrode and charge species.

Fig. 6(a) exhibits the galvanostatic CD curves of all samples between 0 and 0.9 V taken with current density of 0.5 A g^{-1}. As illustrated in Fig. 6, the CD curves of the U-MWNTs and UO-MWNTs show almost triangular shapes, indicating their ideal capacitive performances. Meanwhile, the CD curve of the O-MWNTs shows a significant drop reflecting the larger resistance and poor conductivity of the electrodes. The gravimetric specific capacitance (F g^{-1}) of these electrodes for supercapacitors could be calculated from the CD curves on the basis of Eq. (1), as shown in Fig. 6(b). The specific capacitance for UO-MWNTs is the highest value of 41.5 F g^{-1}; for the U-MWNTs it is 36 F g^{-1} compared to MWNTs. The highest specific capacitance of the UO-MWNTs as a function of the cycle number is presented in Fig. 7. The long term cycle stability of the UO-MWNTs was also estimated by repeating with current density of 0.5 A g^{-1} for 100 cycles. The UO-MWNT electrodes were found to exhibit an excellent stability over all cycle numbers. After the first cycle, the specific capacitance was slightly increased and thereafter, the electrode reached a stable state. After 100 cycles, the capacitance reduced by approximately 8% of the initial specific capacitance, indicating that the UO-MWNTs could be used as electrodes with excellent cycle stability. The decrease in the specific capacitance could be attributed to the swelling and shrinkage during the long term charge/discharge processes [32].

These enhancing capacitive behaviors of nitrogen-containing MWNTs-based electrodes were noted that the electrochemically active nitrogen functional groups are represented by N-6 and N-5 as they are known to possess a negative charge due to the lone electron pair that featured to be conjugated within the π electron system on edge of graphene sheets and thus be electrochemically active site. Also, it has been shown that the pyrone oxygen is the most important oxygen functional groups on carbon with regards to its electrochemical activity [14]. Meanwhile, the XPS analysis clearly shows the presence of N-5 and N-6 functional groups in all the samples, while the N-5 ratios of UO-MWNTs are slightly higher than the U-MWNTs. These nitrogen species are located at the easily accessible edges of graphene layers, and therefore they

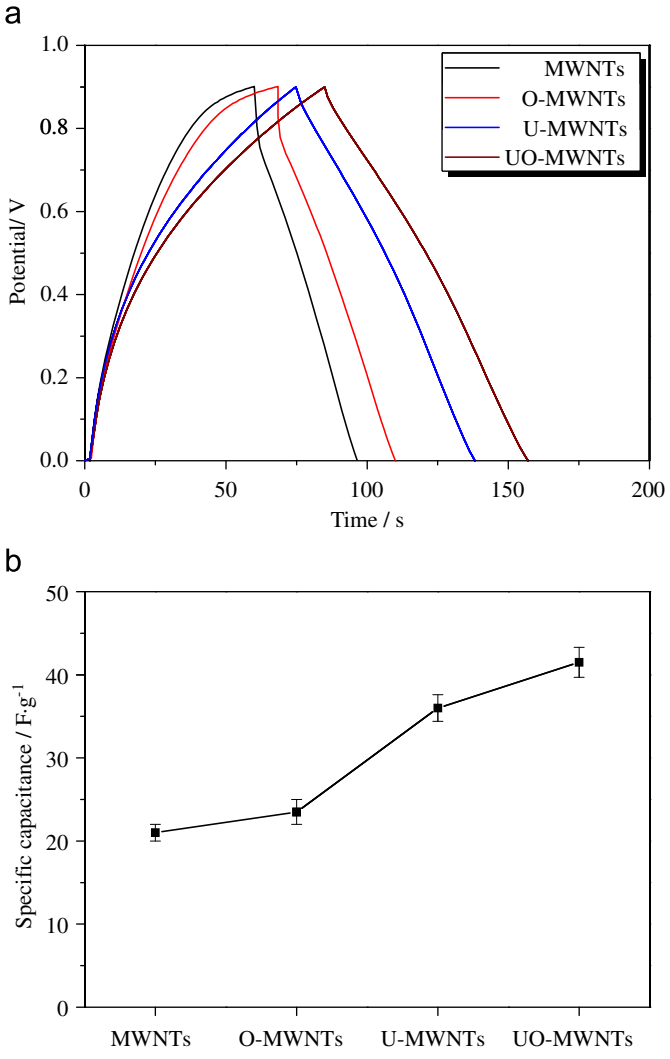

Fig. 6. . (a) Charge–discharge curves of surface treated MWNT electrodes with current density of 0.5 A g^{-1}, and (b) specific capacitance of all electrodes for supercapacitors.

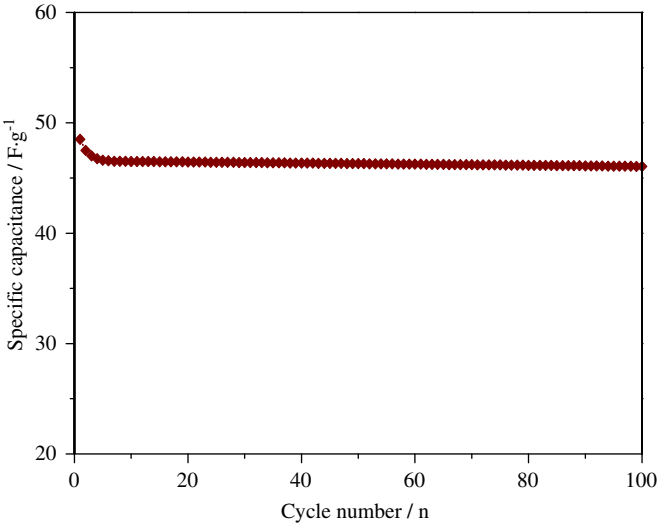

Fig. 7. Specific capacitances of surface treated MWNT electrodes as a function of the cycle number measured with current density of 0.5 A g^{-1}.

can easily improve the specific capacitance with the pseudo-capacitive effect. The N-5 species induces electron donor properties to the layer, and therefore one can reasonably suggest that the protons were attracted to the electrode surface and the pseudo-capacitive effect easily occurred than U-MWNTs. This may be a main reason for the enhanced capacitive behaviors of UO-MWNTs with very poor porosities but with the higher ratios of nitrogen functional groups as compared to the U-MWNTs.

4. Conclusions

In this study, we confirmed that the nitrogen and oxygen functional groups play a prominent role as an excellent support for the electrochemical properties of MWNTs. Although the UO-MWNTs showed damaged structural parameters, the content of nitrogen increased about twice as nitrogen-containing of U-MWNTs with improving capacitive performance. Furthermore, the specific capacitance could be influenced by the surface functional groups, because both oxygen and nitrogen can affect the capacitance uptake by their pseudo-capacitive effect. It was suggested that the N-5 species affected the electron donor acceptor characteristic of carbon materials and that the pseudo-capacitive attraction between the protons of electrolyte and the carbon electrode materials occurred. This was proposed to be the reason for excellent capacitive behaviors of carbon materials in an aqueous electrolyte solution.

Acknowledgments

This work was supported by the IT Industrial Source Technology Development Business of the Ministry of Knowledge Economy, Korea.

References

[1] B.E. Conway, 'Electrochemical supercapacitors' in Scientific Fundamentals and Technological Applications, Kluwer-Plenum Press, NY, 1999.
[2] C. Liu, F. Li, L.P. Ma, H.M. Cheng, Adv. Mater. 22 (2010) E28–E62.
[3] S.G. Lee, K.H. Park, W.G. Shim, M.S. Balathanigaimani, H. Moon, J. Ind. Eng. Chem., 2011, in press.
[4] J. Feng, J. Zhao, B. Tang, P. Liu, J. Xu, J. Solid State Chem. 183 (2010) 2932–2936.
[5] M.K. Seo, S.J. Park, Curr. Appl. Phys. 10 (2010) 241–244.
[6] A. Malak-Polaczyk, C. Matei-Ghimbeu, C. Vix-Guterl, E. Frackowiak, J. Solid State Chem. 183 (2010) 969–974.
[7] Y.J. Kim, Y. Abe, T. Yanagiura, K.C. Park, M. Shimizu, T. Iwazaki, S. Nakagawa, M. Endo, M.S. Dresselhaus, Carbon 45 (2007) 2116–2125.
[8] M.D. Obradović, G.D. Vuković, S.I. Stevanović, V.V. Panic, P.S. Uskoković, A. Kowal, S.Lj. Gojković, J. Electroanal. Chem. 634 (2009) 22–30.
[9] S.Y. Lee, S.J. Park, J. Solid State Chem. 183 (2010) 2951–2956.
[10] Y.S. Yang, C.Y. Wang, M.M. Chen, Z.Q. Shi, J.M. Zheng, J. Solid State Chem. 183 (2010) 2116–2120.
[11] S. Kim, Y. Jung, S.J. Park, Carbon Lett. 10 (2009) 213–216.
[12] B. Xua, F. Wub, Y. Sub, G. Cao, S. Chen, Z. Zhou, Y. Yang, Electrochim. Acta 53 (2008) 7730–7735.
[13] N. Alexeyeva, E. Shulga, V. Kisand, I. Kink, K. Tammeveski, J. Electroanal. Chem. 648 (2010) 169–175.
[14] E. Raymundo-pinero, D. Cazorla-Amorós, A. Linares-Solano, J. Find, U. Wild, R. Schlögl, Carbon 40 (2002) 597–608.
[15] J. Machnikowski, B. Grzyb, J.V. Weber, E. Frackowiak, J.N. Rouzaud, F. Béguin, Electrochim. Acta. 49 (2004) 423–432.
[16] D. Hulicova-Jurcakova, M. Seredych, G.Q. Lu, T.J. Bandosz, Adv. Funct. Mater. 19 (2009) 438–447.
[17] H.-P. Boehm, Carbon 32 (1994) 759–769.
[18] M.A. Montes-Morán, D. Suárez, J.A. Menéndez, E. Fuente, Carbon 42 (2004) 1219–1225.
[19] D. Hulicova-Jurcakova, M. Kodama, H. Hatori, Chem. Mater. 18 (2006) 2318–2326.
[20] E. Frackowiak, G. Lota, J. Machnikowski, C. Vix-Guterl, F. Béguin, Electrochim. Acta 51 (2006) 2209–2214.
[21] B.K. Kim, S.K. Ryu, B.J. Kim, S.J. Park, J. Colloid Interface Sci. 302 (2006) 695–697.
[22] D. Foy, G. Demazeau, P. Florian, D. Massiot, C. Labrugére, G. Goglio, J. Solid State Chem. 182 (2009) 165–171.
[23] F. Kapteijn, J.A. Moulijn, S. Matzner, H.-P. Boehm, Carbon 37 (1999) 1143–1150.
[24] R.C. Bansal, M. Goyal, Activated Carbon Adsorption, Taylor & Francis, FL, 2005.
[25] S.J. Park, S.Y. Jin, J. Colloid Interface Sci. 286 (2005) 417–419.
[26] C.C. Lin, H.C. Huang, J. Power Sources 188 (2009) 332–337.
[27] L.M. Le Leuch, T.J. Bandosz, Carbon 45 (2007) 568–578.
[28] Y. Liu, L. Gao, S. Zheng, Y. Wang, J. Sun, H. Kajiura, Y. Li, K. Noda, Nanotechnology 18 (2007) 365702–365707.
[29] L. Vaisman, G. Marom, H.D. Wagner, Adv. Funct. Mater. 16 (2006) 357–363.
[30] E.J.W. Verwey, J Th., G. Overbeek, Theory of the Stability of Lyophobic Colloids, Elsevier, Amsterdam, 1948.
[31] N.G. Skinner, E.A.H. Hall, Synth. Met. 63 (1994) 133–145.
[32] V. Khomenko, E. Frackowiak, F. Béguin, Electrochim. Acta 50 (2005) 2499–2506.